Supporting Material: Mechanical modulation of receptor-ligand interactions at cell-cell interfaces

Jun F. Allard[1,*], Omer Dushek[2,3,*,‡], Daniel Coombs[4], P. Anton van der Merwe[2]

[1]Department of Mathematics, University of California, Davis
[2]Sir William Dunn School of Pathology, University of Oxford
[3]Centre for Mathematical Biology, University of Oxford
[4]Department of Mathematics and Institute of Applied Mathematics, University of British Columbia, Canada
[*]These authors contributed equally
[‡]Corresponding author

Supporting Material

Parameter estimates.

The eight model parameters along with estimated values are summarized in Table 1. We have used published parameter values where available and varied parameters whose values are presently unknown or have large experimental uncertainties. The diffusion coefficient of membrane-anchored molecules is in the range of $D \sim$0.01 μm^2/s (1). We take the length of LSMs to be $z_p = 50$ nm and the receptor-ligand bond length to be $z_0 = 13$ nm (3, 4). Estimates of k^0_{off} are available for many receptor-ligand interactions and are in the range of 0.01 - 10 s^{-1} (4, 5). The number of LSMs on a typical cell surface is large. For example, the transmembrane molecule CD45 with an ectodomain length of approximately 50 nm is the most abundant cell surface molecule on lymphocytes (4). We take the concentration of LSMs to be $P_0 = 1000$ μm^{-2} (4). The membrane bending stiffness has been variously measured and we take a value of $\kappa_M = 50\,$pN nm (7). Given the uncertainty in k_p, z_0, z_p, and P_0, we systematically vary these.

The two key parameters that are presently unknown are the force parameter (f_B) and the compressional stiffness of LSMs (k_p).

The compressional stiffness of LSMs is presently unknown but as an approximate value, we take $k_p = 0.1\,$pN/nm which was recently reported for ICAM-1 (2). A FRET system, whereby a donor/acceptor pair are placed at the end of the ectodomain and at the membrane, might provide information on the fraction of time the LSM is near the membrane and this quantity is directly related to k_p.

Estimates of f_B are available for a limited number of receptor-ligand interactions but are often in the

range of $f_B \approx 10$ pN (6). This parameter determines the relevant tension scale on which a chemical bond responds and this parameter can be measured using atomic force microscopy or a flow chamber (17). By varying the applied force, such experiments can also validate (or refute) the Bell/Kramer model.

Mechanical quasi-equilibrium

Lateral reorganization of LSMs occurs on timescales ranging from milliseconds (under forces of $f \sim 10\,$pN, $\tau = w/\mu f \sim 1$ millisecond) to seconds (when purely diffusive, $\tau = w^2/D \sim 1$ second). Mechanical relaxation of the membrane and the elastic response of LSMs is rate-limited membrane deformation, with a timescale of microseconds for a free membrane on length scales $< 100\,$nm where hydrodynamic effects are negligible (8, 9). Because of this separation of timescales, we assume the system is in mechanical equilibrium at each instant on the timescale of lateral LSM motion. While more complicated treatments of membrane dynamics, including thermal fluctuations (10, 11) and non-instantaneous (12) and nonlocal (13) dynamics, are possible, we use a simple model that captures the essential physics of the system.

Estimation of attachment timescales

Our initial conditions assume a homogenous distribution of LSM at the time of binding. This is based on the assumption that receptor-ligand binding occurs when the two membranes are in proximity due to fluctuations of the membrane and LSM compression or by an active process, such as a filopodia-like protrusion, that transiently compresses the LSM. Another possibility is that bonds form when there is a region of width $\sim w$ transiently depleted, pre-evacuated, of LSM by diffusion fluctuations. However, here we show that the timescale of formation of pre-evacuated regions is a prohibitively rare event.

We first compute the probability ρ of finding a pre-evacuated patch. The patch is a circle of radius $w \approx 100\,$nm (see Results). The total surface area of the cell is $\sim 30\,\mu$m^2 (4), much larger than the area of the patch. For now, we assume the membrane is a planar disk with radius $l \gg w$, centered on the patch. It contains $n = P_0 \pi l^2$ particles. One particle's probability of being inside the patch is simply the ratio of the area of the patch to the total area, w^2/l^2. Because diffusion is uniform and the particles are assumed not to interact, the probability of all particles being outside the patch is the probability of one particle being outside the patch, multiplied n times, giving

$$\rho_l = \left(1 - \frac{w^2}{l^2}\right)^n = \left(1 - \frac{w^2}{l^2}\right)^{P_0 \pi l^2}. \tag{1}$$

Taking the limit as $l \gg w$ gives $\rho = \exp(-P_0 \pi w^2)$. For parameters in Table 1, this gives $\rho \approx 10^{-14}$. We conclude that the probability of a particular receptor-ligand pair finding an open patch is extremely small.

Because diffusion in this system is ergodic (14), the quantity ρ is also the fraction of time a region is empty. This implies

$$\frac{t_0}{t_0 + t_{ne}} = \rho \tag{2}$$

where t_0 is the mean time the region remains empty and t_n is the mean time the region is non-empty. Here we make a crude estimate of t_{ne}, which represents how long the receptor-ligand pair must wait before a

pre-evacuated region forms, allowing it to bind. Rearranging and expanding for small ρ gives $t_{ne} \approx t_0 \rho^{-1}$. We compute an order-of-magnitude estimate of t_0 by assuming that the membrane surface, with a circular region of radius w removed, has uniform LSM density P_0. The timescale for the empty region to equilibrate to its steady-state density P_0 is $t \sim w^2/D$ from scaling arguments (15), at which point it will contain, on average, $P_0 w^2$ LSM particles. By linear approximation, the first few particles enter after a time $t_0 \sim (1/P_0 w^2)(w^2/D) = 1/(P_0 D)$. This leads to a rough estimate of $t_{ne} \sim 1/(P_0 D)\exp(+P_0 \pi w^2)$. Using parameters from Table 1, this is $t_n \sim 10^{12}$ s. This long time is further suggestion that binding must occur by a process other than LSM pre-evacuation.

An alternative mechanism of binding is the spontaneous (i.e. thermal) compression of all or most LSM in the patch of radius w. This would involve an energy of $\sim k_p z_p^2 \approx 32 k_B T$ for each of $n \approx 31$ particles, requiring $\approx 900 k_B T$, which is exceedingly unlikely to be provided by thermal fluctuations. Taken together, the above estimates suggest an active process is requires to squeeze the LSM and membranes together, allowing for receptor-ligand binding.

Model analysis

The model is described by the drift-diffusion equation Eq. 1 and mechanical energy functional Eq. 3 in the main text. Here we assume radial symmetry and derive nondimensional equations, which we use to perform scaling analysis and numerical simulation.

We define a lateral length scale $w \equiv (\kappa_M/k_P P_0)^{1/4}$ and rescale lateral position to $R = r/w$. Time is rescaled by the diffusive timescale $T \equiv tD/w^2$; LSM concentration by its initial concentration $Q \equiv P/P_0$; energy to the thermal scale $\mathcal{E} = E/k_B T$; and membrane separation z is rescaled to a relative membrane displacement, $Z \equiv (z_P - z)/(z_P - z_0)$. In nondimensional terms, the drift-diffusion equation becomes

$$\frac{\partial Q}{\partial T} = \nabla^2 Q + Pe\, \nabla \cdot (QZ\nabla Z) \tag{3}$$

where $Pe \equiv k_P(z_P - z_0)^2/k_B T$ is the Péclet number describing the relative importance of drift to diffusion, in this case due to LSM compression and thermal motion respectively. The mechanical energy functional becomes

$$\mathcal{E} = \mathcal{E}_0 \iint \frac{1}{2}(\nabla^2 Z)^2 + \frac{1}{2} Q Z^2 da \tag{4}$$

where $\mathcal{E}_0 \equiv \kappa_M (z_P - z_0)^2/(k_B T w^2)$. Imposing radial symmetry leads to

$$\frac{\partial Q}{\partial T} = \frac{1}{R}\frac{\partial}{\partial R}\left(R\frac{\partial Q}{\partial R}\right) + Pe \frac{1}{R}\frac{\partial}{\partial R}\left(QRZ\frac{\partial Z}{\partial R}\right) \tag{5}$$

and $\mathcal{E} = \int_{R_0}^{R_M} \mathcal{H}\, dR$ where

$$\mathcal{H} = 2\pi \mathcal{E}_0 \left(\frac{1}{2}\frac{1}{R}\left(\frac{\partial}{\partial R}\left(R\frac{\partial Z}{\partial R}\right)\right)^2 + \frac{1}{2} QRZ^2\right). \tag{6}$$

The generalized Euler-Lagrange equation to minimize $\mathcal{E}$ is $\delta\mathcal{E}/\delta Z(R) = 0$, which gives

$$QRZ + Z'/R^2 - Z''/R + 2Z''' + RZ^{(iv)} = 0 \tag{7}$$

with boundary conditions $Z(R_0) = 1$, $Z'(R_0) = Z(R_{max}) = Z'(R_{max}) = 0$. The generalized Euler-Lagrange equation also provides a convenient way to compute the tension at the bond site by using the surface term corresponding to $\delta Z|_{R=R_0} = 0$, which gives $F = 2\pi\mathcal{E}_0(RZ''' + Z'' - Z'/R)|_{R=R_0}$.

These results provide the following scaling relations. The lateral width of the membrane deformation zone and radius of LSM depletion is $X \sim 1$, or $x \sim w$. The tension on the bond is $F \sim 2\pi\mathcal{E}_0$ in units of $k_BT/(z_P - z_0)$, or

$$f \sim f^* = 2\pi(z_P - z_0)\sqrt{\kappa_M k_P P_0}. \tag{8}$$

The timescale of LSM evacuation and return are, respectively, $T_{\text{deplete}} \sim 1/Pe$ and $T_{\text{return}} \sim 1$, or, respectively

$$t_{\text{deplete}} \sim \frac{1}{D}\sqrt{\frac{\kappa_M}{k_P P_0}} \cdot \frac{k_BT}{k_P(z_P - z_0)^2}, \qquad t_{\text{return}} \sim \frac{1}{D}\sqrt{\frac{\kappa_M}{k_P P_0}}. \tag{9}$$

The scaling results in Eqs. 8-9 are order-of-magnitude estimates that are confirmed by numerical results (Fig. S2).

Numerical method

To obtain numerical solutions, we discretize space into rings with $\Delta R = 0.1$ and Eq. 5 using a finite area method and forward-Euler for time marching, with time step ΔT determined dynamically by the Courant condition (16). To solve Eq. 7, we use a numerical relaxation scheme with a Newton-Raphson solver at each time step. Simulations are performed in MATLAB (The MathWorks, Natick, MA). We find the solution insensitive to R_0 and R_{max} (provided $R_{max} \gg 1$), thus there is only one significant parameter, Pe. Several quantities summarizing simulation results are shown as a function of Pe in Fig. S2. All results in the main text are taken from these simulations at appropriate values of Pe and converted to physical units.

References

1. Cairo, C. W., R. Das, A. Albohy, Q. J. Baca, D. Pradhan, J. S. Morrow, D. Coombs, and D. E. Golan, 2010. Dynamic regulation of CD45 lateral mobility by the spectrin-ankyrin cytoskeleton of T cells. *J Biol Chem* 285:11392–11401.

2. Burroughs, N. J., K. Köhler, V. Miloserdov, M. L. Dustin, P. A. van der Merwe, and D. M. Davis., 2011. Boltzmann Energy-based Image Analysis Demonstrates that Extracellular Domain Size Differences Explain Protein Segregation at Immune Synapses. *PLoS Comput Biol* 8:e1002076.

3. Springer, T. A., 1990. Adhesion receptors of the immune system. *Nature* 346:425–434.

4. Barclay, A. N., M. H. Brown, S. A. Law, A. J. McKnight, M. G. Tomlinson, and P. A. van der Merwe, 1997. The Leucocyte Antigen Facts Book. Academic Press, San Diego.

5. van der Merwe, P. A., and S. J. Davis, 2003. Molecular interactions mediating T cell antigen recognition. *Annu Rev Immunol* 21:659–684.

6. Schwesinger, F., R. Ros, T. Strunz, D. Anselmetti, H. J. Güntherodt, A. Honegger, L. Jermutus, L. Tiefenauer, and A. Pluckthun, 2000. Unbinding forces of single antibody-antigen complexes correlate with their thermal dissociation rates. *Proc Natl Acad Sci U S A* 97:9972–9977.

7. Raucher, D., T. Stauffer, W. Chen, K. Shen, S. Guo, J. D. York, M. P. Sheetz, and T. Meyer, 2000. Phosphatidylinositol 4,5-bisphosphate functions as a second messenger that regulates cytoskeleton-plasma membrane adhesion. *Cell* 100:221–228.

8. Yeung, A., and E. Evans, 1995. Unexpected dynamics in shape fluctuations of bilayer vesicles. *Journal de Physique II* 5:1501–1523.

9. Seifert, U., and S. Langer, 1994. Hydrodynamics of membranes: the bilayer aspect and adhesion. *Biophysical chemistry* 49:13–22.

10. Dobrowsky, T. M., B. R. Daniels, R. F. Siliciano, S. X. Sun, and D. Wirtz, 2010. Organization of Cellular Receptors into a Nanoscale Junction during HIV-1 Adhesion. *PLoS Computational Biology* 6:e1000855.

11. Krobath, H., G. J. Schutz, R. Lipowsky, and T. R. Weikl, 2007. Lateral diffusion of receptor-ligand bonds in membrane adhesion zones: Effect of thermal membrane roughness. *European Physics Letters* 1–7.

12. Burroughs, N. J., and C. Wülfing, 2002. Differential segregation in a cell-cell contact interface: the dynamics of the immunological synapse. *Biophys J* 83:1784–1796.

13. Veksler, A., and N. S. Gov, 2007. Phase Transitions of the Coupled Membrane-Cytoskeleton Modify Cellular Shape. *Biophys J* 93:3798–3810.

14. Reichl, L., 1998. A modern course in statistical physics. Wiley-Interscience, Hoboken.

15. Schepartz, B., 1980. Dimensional analysis in the biomedical sciences. Thomas, Springfield.

16. LeVeque, R., 1994. Numerical Methods for Conservation Laws. Birkhäuser Verlag, Basel.

17. Bongrand, P., 1999. Ligand-receptor interactions. *Rep. Prog. Phys.* 921–968.

Supplementary Figures

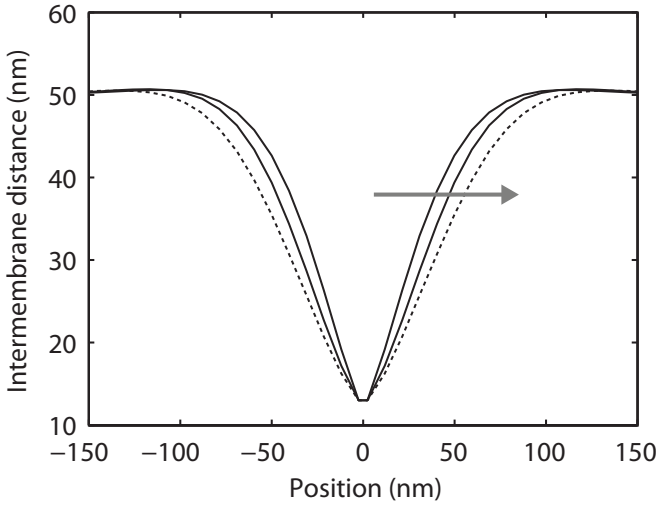

Fig. S1: Intermembrane distance profiles. Shown is the intermembrane distance (y-axis) as a function of the position where 0 nm is the location of the receptor-ligand complex. Profiles are shown for t= $0.00, 0.03,$ and 0.28 s and the grey arrow indicates the direction of increasing time. Note that these small changes in intermembrane distance give rise to large changes in the receptor-ligand bond tension (Fig. 3).

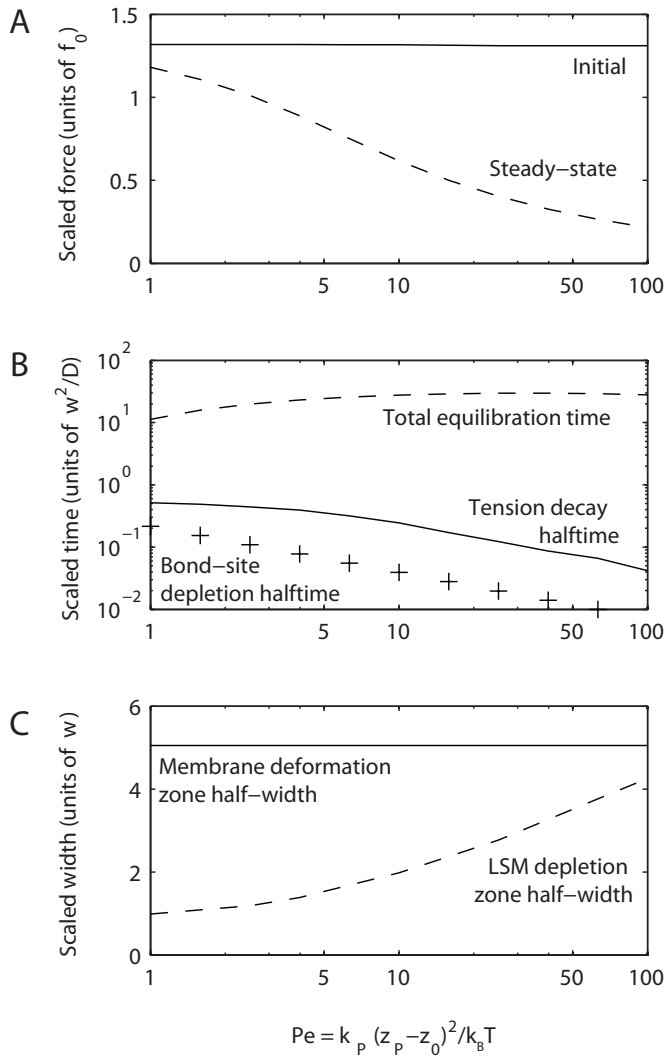

Fig. S2: Numerical simulations of nondimensional model as a function of parameter Pe, the ratio of lateral LSM motion due to compression to thermal diffusion. A) Initial and steady-state tension on bond. B) Total equilibration time, defined as the time until the system changes less than 10^{-3} per time unit; Tension decay halftime; and bond-site depletion half-time, defined as the time for the width of the LSM depletion zone to reach half its steady-state width. C) Width of membrane deformation zone and LSM depletion zone, both defines as full-width at half-max. See Methods for relationship between nondimensional variables and model parameters.

Fig. 1:

Fig. 2:

Fig. 3:

Fig. 4:

Table 1: